Computational Research Progress in Applied Science & Engineering

ISSN 2423-4591

CRPASE Vol. 06(01), 1-8, March 2020

Modeling Performance of Foam-CO2 Reservoir Flooding with Hybrid Machine-learning Models Combining a Radial Basis Function and Evolutionary Algorithms

Seyedeh Raha Moosavi[a], David A Wood[b*], Seyed Abbas Samadani[c]

[a] *Department of Chemical and Petroleum Engineering, Shiraz University, Shiraz, Iran*
[b] *DWA Energy Limited, Lincoln, United Kingdom*
[c] *Persian refinery, Mohr, Fars, Iran*

Keywords

Hybrid radial basis functions,
Evolutionary optimization algorithms,
Prediction performance.

Abstract

The primary objective of this work is to demonstrate that a radial basis function (RBF) optimized with four different evaloutionary optimizers can effectively to predict with high accuracy the oil flow rate and oil recovery factor that results when a crude oil reservoir is flooded with foam-CO2. Injecting CO2 together with surfactant in the form of a foam can significantly improve a crude oil reservoir's sweep efficiency. Here, we couple a radial basis function (RBF) with evolutionary algorithms (particle swarm, imperialist competitive, genetic and teaching-learning based) to develop four hybrid-RBF prediction networks and apply them to predict efficiency of foam-CO2 flooding in oil reservoirs. A dataset with 214 published data records was compiled and used to train, optimize and test the four hybrid-RBF networks. The teaching-learning-based optimized (TLBO-RBF) model achieved the most accurate prediction performance, applied to the full dataset, for estimating oil flow rate (RMSE =0.0031, R2 = 0.997) oil recovery factor (RMSE =0.0175, R2 = 0.999) for the foam-CO2 injection EOR dataset. It can therefore be considered as another algorithm for assessing the impacts of foam-CO2 stimulation of oil-bearing reservoirs efficiently in cases where detailed core measurements are not available.

1. Introduction

A considerable quantity of petroleum is typically left in subsurface reservoirs following primary and secondary production processes [1, 2]. A significant portion of this residual oil can be recovered by applying a range of enhanced oil recovery (EOR) techniques [3]. Chemical flooding of a subsurface reservoir with polymers, surfactant and other chemicals, injection of non-hydrocarbon gases (e.g. carbon dioxide), thermal methods including steam and hot water injection and microbial enhanced oil recovery are among the most widely studied, tested and deployed EOR methods [4, 5].

CO2 injected into sub-surface reservoirs with EOR objectives has significant potential to mitigate the quantity of anthropogenic CO2 that makes its way into the atmosphere while. It can do this while also enhancing oil recovery, thereby boosting energy supply [6, 7, 8].

Foams used for EOR tend to be produced by alternately injecting or co-injecting gases (e.g. nitrogen, CO2, air, natural gas) and foaming agents (an aqueous solution containing a surfactant) into the porous reservoir media. Such foam injection is typically effective in modifying the unfavorable mobility ratio of that porous media. It achieves this by decreasing relative permeability of the pore space and fluids to CO2 and improving the overall sweep efficiency of the reservoir [9, 10]. Many successful field applications of foam injection have demonstrated its ability to increase displacement efficiency compared to basic gas-injection techniques [11, 12].

Designing, managing and running foam-CO2 injection experiments that quantitatively measure oil displacement and production rate from reservoir cores are expensive and time consuming [13, 14]. Hence, the motivation for this study is that there are clear cost advantages and time savings in developing foam-CO2 performance prediction models as way way to reducing the number of expensive experiments that need to be performed [15]. Such models typically evaluate and integrate the performance results of foam-CO2 laboratory-based, core injection tests [16]. Foam-CO2 laboratory tests typically focus on determining the flow rate of oil (Q) through cores of porous media and the recovery of oil from such cores (RF) [17]. These parameters are used to evaluate the performance of foam-CO2 injection applied to

* Corresponding Author:
E-mail address: dw@dwasolutins.com

Received: 16 January 2020; Accepted: 25 February 2020

specific reservoirs [18]. Their values establish whether it is viable and worthwhile applying this EOR method to those reservoirs [19].

Some numerical methods have been developed for predicting either Q or RF for chemical EOR (CEOR) techniques [20], there are few methods that provide precise and fast prediction of oil recovery factor and oil flow rate based on a significant dataset of foam-CO2 injection tests [21]. The primary objective here is to develop and access the performance of efficient and effective machine-learning models which can predict Q and RF related to a compilation of published laboratory data of foam-CO2 injection tests into reservoir cores.

The key novel contribution of this study is that we apply a radial basis function (RBF) hybridized with four evolutionary optimization algorithms (see section 2.3 for a description of the four evolutionary algorithms applied) to develop accurate and robust prediction tools for reliably forecasting the efficiency (i.e., and production rate of oil, Q and oil recovery factor, RF) related to foam-CO2 injection into various oil reservoirs. The prediction accuracy achieved for oil recovery factor and oil flow rate associated with a range of foam-CO2 injection tests using the four hybridized RBF-optimizer models is then compared, and the most accurate model identified..

2. Methodology

2.1. Data Compilation

This computational investigation uses a compiled data set of published results extracted from previous experimental studies of foam-CO_2 reservoir injection core tests compiled by Moosavi et al. [21] from previously published sources: 81 from Zhao [22]; 45 from Ydstebø [23]; 48 from Turta & Singhal [24]; and, 40 from Li et al. [25]. The total data records evaluated is 214, of which 171 data records are dedicated to a training data subset and 43 data records are devoted to a testing data subset. Each data records consists of measured values for six input variables:

- kind of surfactant;
- porosity of reservoir rock (%);
- permeability of reservoir rock (mD);
- pore volume of testing core (cm3);
- oil initial saturation; and,
- the number pore volumes of foam-CO_2 injected.

RF and Q are the associate variables to be predicted by the models. The minimum to maximum range for 6-independent variables associated with core tests are displayed in Table 1.

2.2. Radial Basis Function (RBF)

RBF is one kind of artificial neural network (ANN) algorithm [26], and together with the multi-layer perceptron (MLP) [27], it is one of the most popular ANN methods. ANNs exploiting the RBF algorithm are feed-forward neural networks with a simple network structure with just three-fixed layers: input, hidden, and output. This leads RBF to have simpler structure than an MLP, which typically involves more than one hidden layer, making it easier to train an RBF network than an MLP network. Also, the simple structure of an RBF network makes it easier for it process data records that are outside the ranges covered by the training data subset [28].

Input variable x generates RBF output by applying Eq. (1).

$$y_i(x) = \sum_{i=1}^{m} w_i \, \emptyset \, (\|\mathrm{x} - x_i\|) \quad (1)$$

where

$y_i(x)$= ith output;

m = hidden-layer nodes;

i = ith hidden-layer node;

w_i = weight connecting ith hidden-layer node to ith output;

$\emptyset$ = the radial-basis function (RBF); and,

$\|x - x_i\|$= Euclidean-distance norm of ith output.

RBFs of several different forms could be used. In this study a Gaussian RBF which is commonly exploited for such purposes [28, 29] is applied, as defined by Eq. (2).

$$(\emptyset(\|\mathrm{x} - \mathrm{xi}\|)) = \exp(-\frac{(\|\mathrm{x}-\mathrm{xi}\|)^2}{2\sigma^2}) \quad (2)$$

where

xi = Gaussian-function center; and,

σ = standard deviation or uncertainty range of the Gaussian function.

Applying Eq. (2) means that if the distance of an input from the center of the Gaussian distribution diminishes, then the value of the Gaussian RBF function also declines. The RBF algorithm defined in terms of Eqs. (1) and (2) can effectively derive a global optimal solution by adjusting the hidden-layer nodes' weights (W) and biases (b) to minimize mean square error (MSE) of the predicted versus laboratory-test values of its dependent variables (Q and RF). In its basic form the algorithm seeks this minimum MSE solution with the aid of a linear optimization method. In order to improve the optimization process employed by the RBF network, several evolutionary optimization algorithms (described in the following sections) are tested here to establish their ability to improve upon the performance of the basic linear optimizer.

2.3. Hybridizing the RBF Network with Evolutionary Optimization Algorithms

2.3.1. Genetic Algorithm

Genetic optimization algorithms (GA) are now extensively applied to solve a varied range of non-linear technical problems with single and multiple objective functions [31]. Random chromosomal selection processes analogous to those involved in biological genetic evolution are exploited to generate a population of feasible solutions. The effective genetic processes or operators involving mutation and crossover are employed in GA.

Table 1. 6-metric ranges for foam-CO_2-injection dataset used for EOR tests compiled from four identified published sources.

Type of Surfactant	Porosity (%)	Permeability (mD)	Initial Oil in Place Saturation (%)	Injected Pore Volume of Foam	Total Core Pore Volume (cm^3)	Number of Data Records	References
Bio-Terge AS-40	25.8-34.8	8.5-28.2	94-97	0.3-18	45-49	42	Zhao, 2017 [22]
Triton X-100	23.6-34.8	9-28.2	94-97	0.2-27	44-49	45	Ydstebø, 2013 [23]
VT-90	24.1-34.8	11-28.2	94-97	0.2-23	47-49	40	Li et al., 2010 [25]
Brine	27-34.8	10.5-28.2	94-97	0.2-16	46-49	39	Zhao, 2017 [22]
AOS C14/16	30-34.8	8.5-28.2	94-97	0.2-34	47-49	48	Turta & Singhal, 2002 [24]

The GA procedure commences with the primary chromosomes (independent variables), the variable values are then selected using random probability distributions between 0 and 1. This crossover probability applied to generate individual solutions for the next generation from high-ranking parent solutions is influenced by the GA control variables mutation factor (MF) and crossover factor (CF), which can be varied as the generations evolve to become more focused or search more broadly.

2.3.2. Imperialist Competitive Algorithm (ICA)

This algorithm exploits processes analogous to the observed political competition processes between a colony and its governing imperialistic body [32]. ICA in a way typical of other optimization algorithms commences with an primary randomly-selected population of artificial "countries". Two types of countries are designated: colonies and imperialist powers and the algorithm evolves based on the imperialistic competition that ensues between more powerful (i.e. those with more attractive fitness functions) and less powerful (those with less attractive fitness functions) countries. The imperialists "countries" are more powerful and therefore control empires with more "colonies" and continuously strive to obtain more colonies and increase their power. On the other hand, weak imperialist countries progressively lose their empires of colonies as the ICA algorithm's iterations progress and those weak empires ultimately collapse. As the algorithm evolves, the colonies are gradually accumulated by the most powerful imperialist country into a single dominant empire, which eventually controls all the available colonies. In circumstances where a colony achieves a more powerful position than its imperialist power, the power status of the imperialist country and its stronger colony are interchanged.

2.3.3. Particle Swarm Optimization (PSO)

PSO is an alternative optimization algorithm using a probabilistic approach first established by Eberhart & Kennedy (1995) [33]. It mimics the interactions of fish in shoals, insects in swarms or birds in flocks. Individual swarm particles represent potential objective function solutions to the optimization goal. A randomly-selected initial population of particles is activated to broadly search the feasible solution space [34, 35]. In each iteration of the PSO algorithm, a fitness test values for the solution associated with each particle is evaluated. Based on the fitness test scores the position in the feasible solution space of each particle is adjusted based on two criteria: 1) the locally best position for a particle in the current generation / iteration; and, 2) the globally best position for a particle achieved in the current and all previous iterations of the algorithm. This approach enables the PSO algorithm to explore local and global minima in the feasible solution space [36]. The algorithm essentially exploits the fitness test as its objective function to evaluate the suitability of each particle solution and progressively adjusts each particle's position based on that information for each subsequent iteration. It periodically replaces the global best particle solution found as the iterations progress [37].

2.3.4. Teaching-learning-based Optimization (TLBO)

The TLBO algorithm, derived by Rao et al. [38] and refined by Murty et al. [39], offers an alternative population-based, nature-inspired optimization method. The population involved in the TLBO algorithm is a group or class of learners of user-defined number of individuals. For the foam-CO_2 dataset evaluated here the initial population involves 220 individuals. Two distinct types of learning are involved in the TLBO algorithm: 1) teacher stage - learning from the teacher; and 2) learner stage - learning from other individual learners. Learners' grades or the fitness of their solutions are used to assess the quality of the teacher. Consequently, the teacher teaches the learners so that they achieve better results or fitter solutions. Learners are also able to learn by interactions with each other to boost the compatibility of their solutions. The best prevalent solution in the whole population is assigned the teacher role in each iteration of the algorithm.

As an alternative to RBF optimized with evolutionary algorithms, there is the possibility of applying other machine learning algorithms such as neural networks combined with various fuzzy hierarchy algorithms [40-44]. Future studies will compare the prediction accuracy of such alternatives with the algorithms evaluated here.

3. Statistical Measures of Prediction Accuracy Applied Page Limitation

Five prediction-accuracy statistics are calculated to examine the estimation efficiency of the developed hybrid RBF networks. These measures enable the accuracy of laboratory-measured versus predicted outputs (Q and RF) to be compared. These five statistical measures of accuracy are:

A. Coefficient of determination:

$$R^2 = 1 - \frac{\sum_{i=1}^{N}(out_i^{real} - out_i^{predicted})^2}{\sum_{i=1}^{N}(out_{ave}^{real} - out_i^{predicted})^2} \quad (3)$$

B. Mean squared error:

$$MSE = \frac{1}{N}\sum_{i=1}^{N}(out_i^{real} - out_i^{predicted})^2 \quad (4)$$

C. Root mean squared error:

$$RMSE = (\frac{1}{N}\sum_{i=1}^{N}(out_i^{real} - out_i^{predicted})^2)^{1/2} \quad (5)$$

D. Average absolute relative deviation:

$$AARD = \frac{100}{N}\sum_{i=1}^{N}\left|\frac{out_i^{real} - out_i^{predicted}}{out_i^{real}}\right| \quad (6)$$

where
N = total number of data records;
out_i^{real} = dependent-variable measured values for each data record *i;*
$out_i^{predicted}$ = dependent-variable predicted values for data record *i*; and,
out_{ave}^{real} = Mean of dependent-variable measured values for the dataset as a whole.

E. Standard deviation (SD)

4. Results

4.1. Statistical Accuracy Achieved by the Four Hybrid-RBF Models Developed

Four hybrid RBF neural network models are developed and evaluated to predict the foam-CO_2 injection EOR dependent variables RF and Q. The four hybrid models are:

- GA-RBF
- PSO-RBF
- ICA-RBF
- TLBO-RBF

Each model hybridizes one of the non-linear optimization algorithms an RBF.

Each algorithm evaluates the compiled 214-record dataset of experimental foam-CO2 laboratory core-injection tests described in section 2.1. 80% of the data records in the full dataset are devoted to the training subset for each network, the remaining 20% of data records are allocated to a testing subset. That testing subset provides an independent performance-accuracy test of each hybrid-RBF network once it has been trained.

RBF network component of each hybrid algorithm has a structure involving 38 neurons in its hidden layer. That number of neurons was selected based on sensitivity analysis considering the five statistical prediction performance measures described in section 3.

The statistical accuracy achieved by each hybrid-RBF network is affected by the specific evolutionary algorithms. They optimize the values for the weights (W) and biases (b) applied to the network nodes. Table 2 is given the results of the statistical precision associating with RF and Q estimations for the four distinct optimized hybrid-RBF networks evaluated. These results reveal that all the optimized hybrid-RBF networks accurately predict the dependent variables. However, the TLBO-RBF network achieved the highest prediction accuracy.

4.2. Comparison of the RF and Q predictions Made by the Four Hybrid-RBF Models

The trained and optimized hybrid-RBF models are applied to predict Q and RF in autonomous testing subsets to ascertain their estimation accuracies (Table 2). Once the precision is established with the testing-subset data, each trained hybrid-RBF is deployed to estimate Q and RF for the full dataset (Table 2). Figure 1 compares predicted and measured dependent variable values across the full dataset revealing good agreement across the entire data range evaluated. These plots show close agreement between predictions and experimental data for foam-CO2 tests.

Figure 2 (for Q) and Figure 3 (for RF) further demonstrate the dependent-variable prediction accuracy achieved by each of the four hybrid-RBF network models based on training-subset and testing-subset prediction results. Figure 2 show close agreement between predictions and experimental data for foam-CO2 tests, with two obvious outlying predictions by the ICA-RBF model and one obvious outlying prediction by the PSO-RBF model. Figure 3 show close agreement between predictions and experimental data for foam-CO2 tests, with no obvious outlying predictions for any of the four models evaluated.

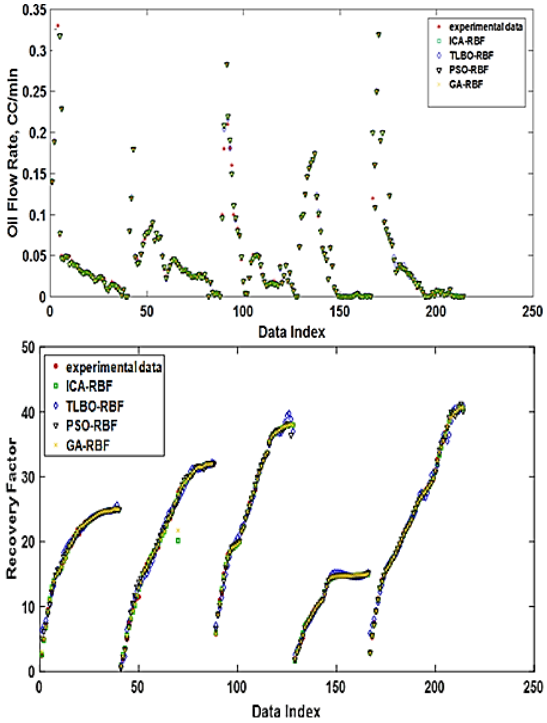

Figure 1. Comparisn of oil flow rate (Q) and recovery factor (RF) values predicted by RBF neural network coupling with evolutionary algorithm and experimentally-measured values versus the index number assigned to specific records.

5. Discussion

5.1. Average Absolute Relative Deviation Achieved by Each Hybrid-RBF Model

Figure 4 (for Q) and Figure 5 (for RF) compare AARD% values for each of the hybrid-RBF models evaluated. These figures highlight the superior accuracy achieved by the TLBO-RBF in predicting Q and RF compared to the other hybrid models.

For computational efficiency comparisons, the processing times for the four hybrid-RBF networks are listed in Table 3. TLBO-RBF shows the minimum calculation time of the four methods. All methods were evaluated using a computer equipped with the same processing unit: Intel(R) Core™ i7 2630QM CPU @ 2.00 GHz. Algorithms for the four hybrid-RBF methods are coded with MatLab software. The TLBO-RBF model required a shorter run time than the other three models.

Table 2. Prediction accuracy assessment for Q and RF by four hybrid RBF networks compared for tuning, testing subsets and the full dataset including all data records.

Model type	Dataset	Recovery factor (RF)				Oil flow rate (Q), CC/min			
		%AARD	MSE	^{r}R	RMSE	%AARD	MSE	^{r}R	RMSE
GA-RBF	Training	2.1	E-049.20	0.998	0.0303	2.3	E-051.16	0.994	0.0034
	Testing	2.8	E-031.80	0.993	0.0424	2.9	E-051.75	0.989	0.0041
	Full dataset	2.4	E-049.50	0.996	0.0308	2.5	E-051.32	0.992	0.0036
PSO-RBF	Training	2.6	E-049.80	0.996	0.0305	2.8	E-051.63	0.992	0.004
	Testing	3.1	E-033.40	0.991	0.0583	3.2	E-052.12	0.986	0.0047
	Full dataset	2.9	E-031.30	0.994	0.0363	3	E-051.82	0.991	0.0042
ICA-RBF	Training	2.2	E-031.50	0.994	0.0387	2.4	E-051.02	0.99	0.0031
	Testing	3.2	E-035.60	0.99	0.0748	3.3	E-052.01	0.981	0.0047
	Full dataset	2.7	E-031.10	0.993	0.0331	2.9	E-051.13	0.989	0.0033
TLBO-RBF	Training	0.8	E-043.20	0.999	0.0173	1.1	E-069.20	0.998	0.003
	Testing	1.2	E-045.70	0.998	0.0244	1.7	E-051.03	0.993	0.0032
	Full dataset	0.9	E-043.30	0.999	0.0175	1.5	E-069.80	0.997	0.0031

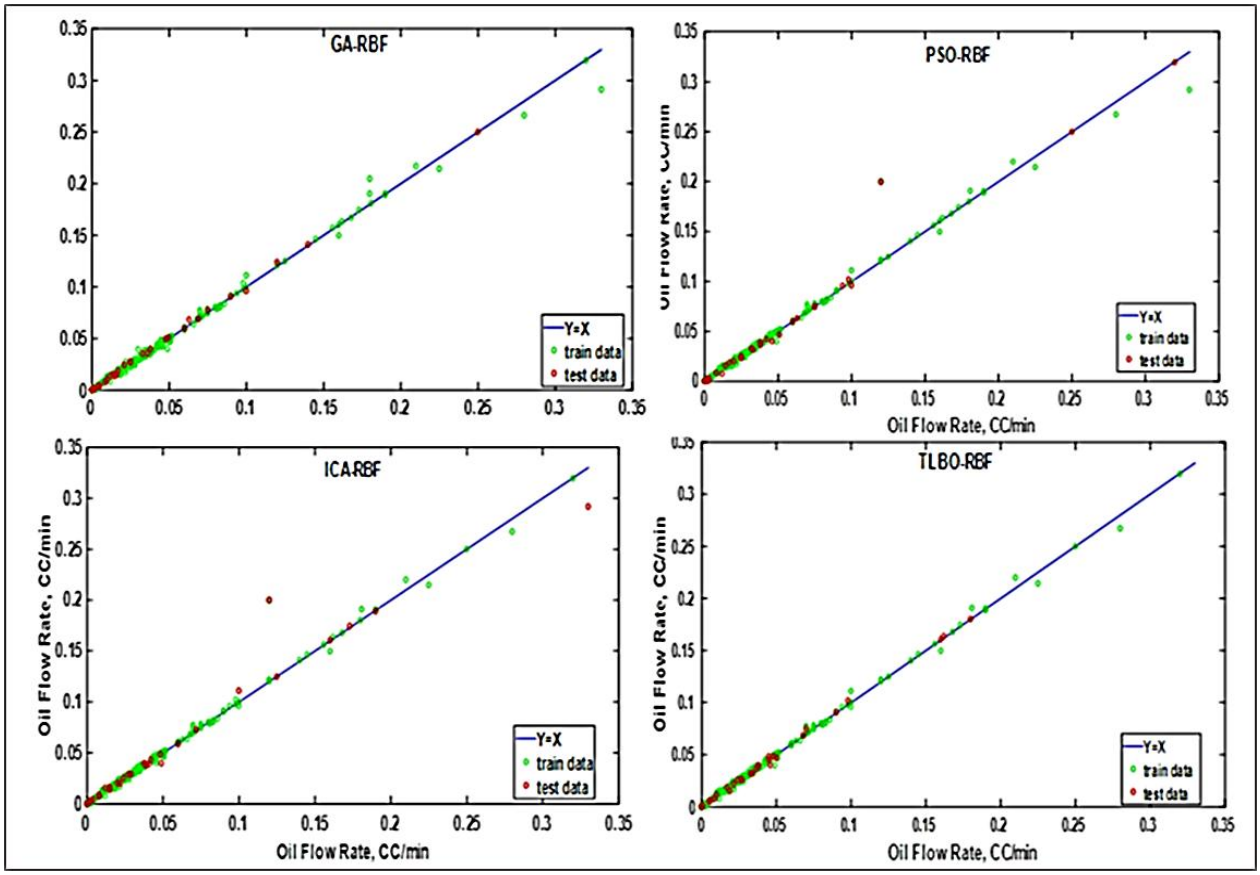

Figure 2. Predicted versus measured values for oil flow rate (Q) derived by the four hybrid-RBF neural networks for training subset (green circles) and testing subset (red circles).

Table 3. Computational efficiency in terms of calculation speed.

Method Solution	Run Time (Seconds)
TLBO-RBF	45.68
GA-RBF	58.34
RBF -ICA	118.49
RBF -PSO	134.87

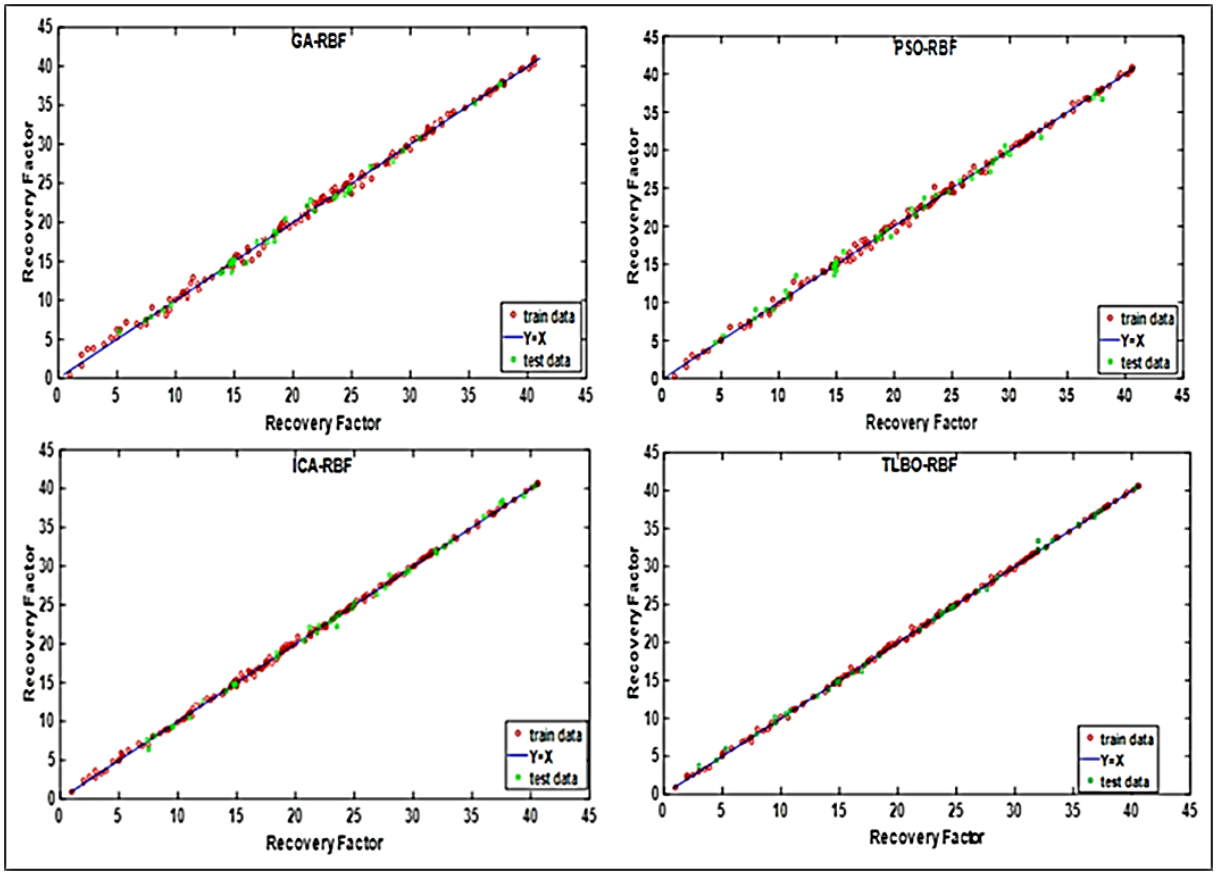

Figure 3. Predicted versus measured values of oil recovery factor (RF) derived by the four hybrid-RBF neural networks for training subset (green circles) and testing subset (red circles).

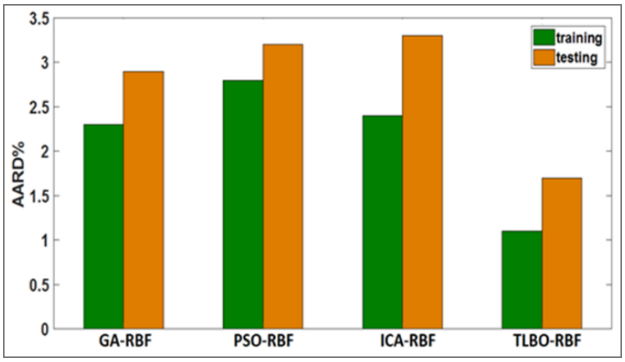

Figure 4. Calculated average absolute relative deviation (AARD%) for oil flow rate (Q), CC/min achieved by each of the four hybrid-RBF models.

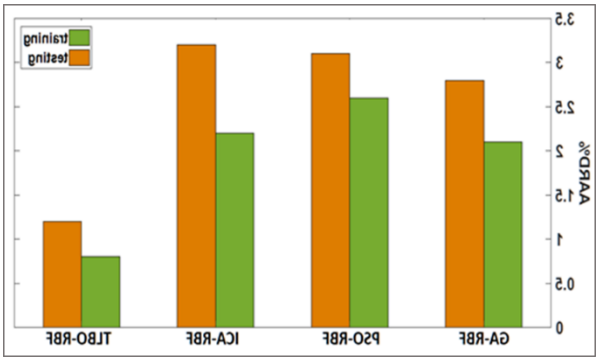

Figure 5. Calculated average absolute relative deviation (AARD%) for oil recovery factor (RF) achieved by each of the four hybrid-RBF models.

5.2. Input-variable Influences on Q and RF Predictions

The foregoing analysis demonstrates that all four hybrid-RBF models provide impressive prediction accuracy of foam-CO_2 injection, and the superior performance of the TLBO-RBF model. Nevertheless, it is useful to establish the relative contributions of each input variable in these models to achieving their prediction performance for Q and RF. An evaluation of a relevancy factor (r) [45] for each input variable with its magnitude calculated with Eq. (7) provides such insight.

$$r = \frac{\sum_{i=1}^{n}(X_{k,i}-\overline{X_k})(Y_i-\overline{Y})}{\sqrt{\sum_{i=1}^{n}(X_{k,i}-\overline{X_k})^2 \sum_{i=1}^{n}(Y_i-\overline{Y})^2}} \quad (7)$$

where

$X_{k,i}$ = ith data record value for kth input metric;

$\overline{X_k}$ = mean kth input metric;

Y_i = ith prediction;

$\overline{Y}$ = mean-predicted value;

n = total data records.

r values calculated with Eq. (7) are constrained between -1 and +1. High r values associated with an input variable identify that specific input variable is having a substantial impact on the dependent-variable predictions. Positive r values occur when increases in input variable values lead to an increase in dependent variable values. On the other hand, negative r values occur when increases in input variable

values lead to a decrease in dependent variable values. Calculated in this way r reveals those input variables that are most influential on dependent variable predictions.

Figure 6 displays the relevancy factor calculations for each input variable on Q and RF predictions for the high-performing TLBO-RBF model. This analysis indicates that the pore-volume injection magnitude of CO_2 is much more influential on the Q and RF estimations than the other five variables involved. On the contrary, among all six independent variables involved, the percentage in-place oil saturation (initial) has the lowest influence on predicted Q and RF values.

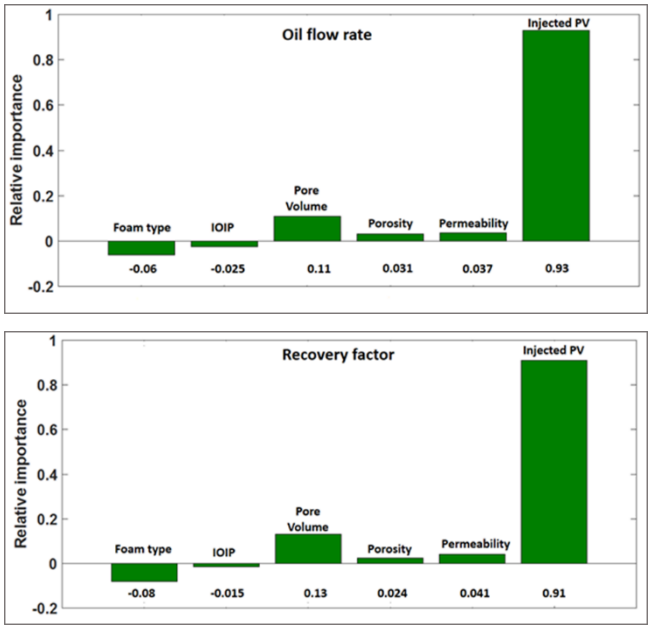

Figure 6. Input-variables influences in determining the predictions of oil flow rate (Q) and recovery factor (RF) from the foam-CO_2 injection EOR dataset for the TLBO-RBF model.

6. Conclusions

Conducting laboratory experiments to assess the oil production and recovery factor performance associated with injecting foam-CO2 into specific oil reservoirs is expensive and time consuming. Simulation techniques can be a viable alternative if they can provide accurate predictions of flow rate and recovery factor from a standard set of input variables. CO2 injection into sub-surface oil reservoirs is a well-established technique for enhancing oil recovery. However, as CO2 is a gas and gases have low reservoir-sweep efficiency, injecting CO2 together with surfactant in the form of a foam can significantly improve its reservoir sweep efficiency. So, foam-CO2 flooding of petroleum reservoirs is a highly effective method able to enhance oil recovery from many reservoirs.

Four optimized hybrid-RBF artificial neural networks demonstrate highly accurate estimation accuracy for oil flow rate (Q) and oil recovery factor (RF) in enhanced-oil-recovery conditions with a 214-record dataset of foam-CO2 injection tests into oil-saturated cores. Each data record evaluated includes values for six independent input variables in addition to Q and RF values. Eighty percent of the data records were used to train the hybrid-RBF networks. Twenty percent of the data records were held independently of the training subset in order to test the trained networks.

High full-dataset prediction accuracy was attained by all four hybrid-RBF models. However, the teaching learning based optimization hybrid model (TLBO-RBF) achieved the greatest accuracy in predicting Q (RMSE =0.0031, R2 = 0.997) and RF (RMSE =0.0175, R2 = 0.999) demonstrating its excellent prediction capabilities for the foam-CO_2 injection EOR dataset studied. Based on this prediction performance, we conclude that the TLBO-RBF offers the best potential to be exploited in predicting, on an unsupervised basis, the foam-CO_2 enhanced oil recovery potential of porous oil-bearing formations with no test data on cores available.

Conflict of Interest

The authors declare that they have no conflict of interest.

Funding

The authors declare that they have received no funding to support this study.

References

[1] V. Alvarado, E. Manrique, Enhanced oil recovery: an updated review. Energies 3 (2010) 1529–1575.
[2] S. Thomas, Enhanced oil recovery-an overview. Oil & Gas Science and Technology-Revue de l'IFP 63 (2008) 9–19.
[3] L.W. Lake, R.T. Johns, W. R. Rossen, G. A. Pope, Fundamentals of enhanced oil recovery. E-book Society of Petroleum Engineers. 2014.
[4] A. Muggeridge, A. Cockin, K. Webb, H. Frampton, I. Collins, T. Moulds, P. Salino, Recovery rates, enhanced oil recovery and technological limits, Phil. Trans. R. Soc. A. 2014.
[5] X. Sun, Y. Zhang, G. Chen, Z. Gai, Application of nanoparticles in enhanced oil recovery: a critical review of recent progress. Energies 10 (2017).
[6] M. Nobakht, S. Moghadam, Y. Gu, Effects of viscous and capillary forces on CO2 enhanced oil recovery under reservoir conditions. Energy & Fuels 21 (2007) 3469–3476.
[7] Z. Dai, R. Middleton, H. Viswanathan, J. Fessenden-Rahn, J. Bauman, R. Pawar, S.Y. Lee, B. McPherson, An integrated framework for optimizing CO2 sequestration and enhanced oil recovery. Environmental Science & Technology Letters 1 (2013) 49–54.
[8] F.A. Rahman, MMA Aziz, R. Saidur, WA Bakar, MR Hainin, R. Putrajaya, NA.Hassan, Pollution to solution: Capture and sequestration of carbon dioxide (CO2) and its utilization as a renewable energy source for a sustainable future. Renewable and Sustainable Energy Reviews 71 (2017) 112–126.
[9] C. Da, Z. Xue, A.J. Worthen, A. Qajar, C. Huh, M. Prodanovic, KP. Johnston, Viscosity and stability of dry CO2 foams for improved oil recovery. In SPE Improved Oil Recovery Conference. 11-13 April, Tulsa, Oklahoma, USA. Society of Petroleum Engineers. SPE-179690-MS (2016).
[10] ZP Alcorn, SB Fredriksen, M. Sharma, MA Fernø, A. Graue, CO2 Foam EOR Field Pilot-Pilot Design, Geologic and Reservoir Modeling, and Laboratory Investigations. In IOR 2017-19th European Symposium on Improved Oil Recovery, (2017).
[11] A. Andrianov, R. Farajzadeh, NM. Mahmoodi, Talanana M, Zitha PL. Immiscible foam for enhancing oil recovery: bulk and porous media experiments. Industrial & Engineering Chemistry Research 51 (2012) 2214–2226.
[12] Y Zhang, X. Yue, J. Dong, L. Yu, New and effective foam flooding to recover oil in heterogeneous reservoir. In SPE/DOE Improved Oil Recovery Symposium 3-5 April, 2000 Tulsa, Oklahoma, U.S.A. Society of Petroleum Engineers. SPE-59367-MS, (2000).

[13] J. Sheng, Enhanced oil recovery field case studies. Gulf Professional Publishing. eBook , 2013.

[14] MM Al-Dousari, AA Garrouch, An artificial neural network model for predicting the recovery performance of surfactant polymer floods. Journal of Petroleum Science and Engineering. 109 (2013) 51–62.

[15] N. Kalyanaraman, C. Arnold, A. Gupta, JS Tsau, RB. Ghahfarokhi, Stability improvement of CO2 foam for enhanced oil-recovery applications using polyelectrolytes and polyelectrolyte complex nanoparticles. Journal of Applied Polymer Science 134 (2016).

[16] X. Xu, A. Saeedi, K. Liu, An experimental study of combined foam/surfactant polymer (SP) flooding for carbon dioxide-enhanced oil recovery (CO2-EOR), Journal of Petroleum Science and Engineering 149 (2017) 603–611.

[17] M. Simjoo, PL. Zitha, New Insight into Immiscible Foam for Enhancing Oil Recovery, Flow and Transport in Subsurface Environment (2018) 91–115.

[18] S. Ahmed, KA. Elraies, IM Tan, MR. Hashmet, Experimental investigation of associative polymer performance for CO2 foam enhanced oil recovery. Journal of Petroleum Science and Engineering 157 (2017) 971–979.

[19] Y. Zeng, K. Ma, R. Farajzadeh, M. Puerto, SL. Biswal, Hirasaki GJ. Effect of Surfactant Partitioning Between Gaseous Phase and Aqueous Phase on CO2 Foam Transport for Enhanced Oil Recovery. Transport in Porous Media 114 (2016) 777–793.

[20] MA Ahmadi, M. Pournik, A predictive model of chemical flooding for enhanced oil recovery purposes: Application of least square support vector machine, Petroleum 2 (2016) 177–182.

[21] SR. Moosavi, DA. Wood, MA. Ahmadi, A. Choubineh, ANN-based prediction of laboratory-scale performance of co2-foam flooding for improving oil recovery. Natural Resources Research 28 (2019) 1619–1637.

[22] J. Zhao, Comprehensive Experimental Study on Foam Flooding for Enhancing Heavy Oil Recovery, Master's Thesis, Faculty of Graduate Studies and Research, University of Regina, 2017.

[23] T. Ydstebø Enhanced Oil Recovery by CO2 and CO2-Foam in Fractured Carbonates, MSc. thesis, The University of Bergen, 2013.

[24] AT. Turta, Singhal AK. Field foam applications in enhanced oil recovery projects: screening and design aspects. Journal of Canadian Petroleum Technology 41 (2002).

[25] RF. Li, W. Yan, S. Liu, G. Hirasaki, CA. Miller, Foam mobility control for surfactant enhanced oil recovery. SPE Journal 15 (2010) 928–942.

[26] DS. Broomhead, D. Lowe, Radial basis functions, multi-variable functional interpolation and adaptive networks, Royal Signals Radar Establishment, Malvern, United Kingdom, Memorandum (1988) 1–34.

[27] SS. Haykin, Neural networks and learning machines, third edition, Pearson Prentice Hall, 2009.

[28] K. Keshmiri, A. Vatanara, Y.Yamini, Development and evaluation of a new semi-empirical model for correlation of drug solubility in supercritical CO2, Fluid Phase Equilibria, (2014) 18–26.

[29] J. Chrastil, Solubility of solids and liquids in supercritical gases. The Journal of Physical Chemistry 86 (1982) 3016–3021.

[30] R. Eghtedaei, M. Abdi-Khanghah, BS. Najar, A. Baghban, Viscosity estimation of mixed oil using RBF-ANN approach. Petroleum Science and Technology 35 (2017) 1731–1736.

[31] V. Mansouri, R. Khosravanian, DA Wood, BS. Aadnoy, 3-D well path design using a multi- objective genetic algorithm. Journal of Natural Gas Science and Engineering 27 (2015) 219–235.

[32] E. Atashpaz-Gargari, C. Lucas, Imperialist competitive algorithm: an algorithm for optimization inspired by imperialistic competition, Evolutionary computation,. CEC 2007. IEEE Congress on Evolutionary Computing. IEEE (2007) 4661–4667.

[33] R. Eberhart, J. Kennedy, A new optimizer using particle swarm theory. in Symposium on Micro Machine and Human Science. Japan: Nagoya, Piscataway, NJ, (1995) 39–43.

[34] JE Onwunalu, LJ. Durlofsky, Application of a particle swarm optimization algorithm for determining optimum well location and type. Comput Geosc. 14 (2010) 183–98.

[35] A. Sharma, G. Onwubolu, Hybrid particle swarm optimization and GMDH system. In: Onwubolu GC, editor. Hybrid self-organizing modeling systems. Berlin, Heidelberg: Springer Berlin Heidelberg; (2009) 193–231.

[36] A. Atashnezhad, DA Wood, A. Fereidounpour, R. Khosravanian, Designing and optimizing deviated wellbore trajectories using novel particle swarm algorithms, Journal of Natural Gas Science and Engineering 21 (2014) 1184–1204

[37] O. Castillo, Type-2 Fuzzy Logic in Intelligent Control Applications, Springer, 2012

[38] RV Rao, VJ Savsani, DP. Vakharia, Teaching–learning-based optimization: an optimization method for continuous non-linear large-scale problems. Information Sciences 183 (2012) 1–5.

[39] MR Murty, A. Naik, JVR Murthy, PVGD Reddy, SC Satapathy, K. Parvathi, Automatic clustering using teaching-learning-based optimization. Appl Math., 5 (2014) 1202–11.

[40] M. Shirmohammadli, A Hybrid Method for Fault Location on VSC-HVDC System Using ANFIS with New Training Algorithm and Hilbert-Huang Transform. Computational Research Progress in Applied Science & Engineering 5 (2019).

[41] A. Addeh, AA Kalteh, A. Koochaki, Hybrid Method for Fault Location in HVDC-Connected Wind Power Plants Using Optimized RBF Neural Network and Efficient Features. Computational Research Progress in Applied Science & Engineering 4 (2018) 6–12.

[42] A. Soltani, Sh. Azadi, SB Choi, A. Bagheri, Performance Evaluation of Semi-Active Vehicle Suspension System Utilizing a New Adaptive Neuro-Fuzzy Controller Associated with Wavelet Transform. Computational Research Progress in Applied Science & Engineering 4 (2018) 55–61.

[43] RZ. Shourabi, MR Moradian, An Intelligent Method Based on Model Predictive Torque Control and Optimized ANFIS for Induction Motor Speed Control. Computational Research Progress in Applied Science & Engineering 4 (2018) 94–100.

[44] H. Ziari, A. Amini, A. Saadatjoo, SM Hosseini, VNM.Gilani, A Prioritization Model for the Immunization of Accident Prone Using Multi-criteria Decision Methods and Fuzzy Hierarchy Algorithm. Computational Research Progress in Applied Science & Engineering 3 (2017) 123–131.

[45] S. Hajirezaie, A. Hemmati-Sarapardeh, AH Mohammadi, M. Pournik, A. Kamari, A smooth model for the estimation of gas/vapor viscosity of hydrocarbon fluids. Journal of Natural Gas Science and Engineering 26 (2015) 1452–1459.